






Time-reversal symmetry breaking in the noncentrosymmetric Zr_3Ir superconductorT. Shang ^{1,*}, S. K. Ghosh,^{2,†} J. Z. Zhao,³ L.-J. Chang ⁴, C. Baines,⁵ M. K. Lee,⁴ D. J. Gawryluk ¹, M. Shi,⁶ M. Medarde,¹ J. Quintanilla ² and T. Shiroka ^{7,5}¹Laboratory for Multiscale Materials Experiments, Paul Scherrer Institut, CH-5232 Villigen PSI, Switzerland²School of Physical Sciences, University of Kent, Canterbury CT2 7NH, United Kingdom³Co-Innovation Center for New Energetic Materials, Southwest University of Science and Technology, Mianyang 621010, People's Republic of China⁴Department of Physics, National Cheng Kung University, Tainan 70101, Taiwan⁵Laboratory for Muon-Spin Spectroscopy, Paul Scherrer Institut, CH-5232 Villigen PSI, Switzerland⁶Swiss Light Source, Paul Scherrer Institut, CH-5232 Villigen PSI, Switzerland⁷Laboratorium für Festkörperphysik, ETH Zürich, CH-8093 Zurich, Switzerland

(Received 21 September 2019; accepted 1 July 2020; published 17 July 2020)

We report the discovery of Zr_3Ir as a structurally different type of unconventional noncentrosymmetric superconductor (with $T_c = 2.3$ K), here investigated mostly via muon-spin rotation/relaxation (μ SR) techniques. Its superconductivity was characterized using magnetic susceptibility, electrical resistivity, and heat capacity measurements. The low-temperature superfluid density, determined via transverse-field μ SR and electronic specific heat, suggests a fully gapped superconducting state. The spontaneous magnetic fields, revealed by zero-field μ SR below T_c , indicate the breaking of time-reversal symmetry in Zr_3Ir and hence the unconventional nature of its superconductivity. By using symmetry arguments and electronic-structure calculations we obtain a superconducting order parameter that is fully compatible with the experimental observations. Hence, our results clearly suggest that Zr_3Ir represents a structurally different member of noncentrosymmetric superconductors with broken time-reversal symmetry.

DOI: [10.1103/PhysRevB.102.020503](https://doi.org/10.1103/PhysRevB.102.020503)

Unconventional superconductors, in addition to $U(1)$ gauge symmetry, also break other types of symmetry [1,2]. Among them, the breaking of time-reversal symmetry (TRS) below T_c has been widely studied, in particular by means of zero-field muon-spin relaxation (ZF- μ SR). As a very sensitive technique, μ SR is able to detect the tiny spontaneous magnetic fields appearing below the onset of superconductivity (SC). Unconventional superconductors known to exhibit TRS breaking include, e.g., Sr_2RuO_4 [3], $PrOs_4Sb_4$ [4], UPT_3 [5], $LaNiGa_2$ [6], $LaNiC_2$, La_7T_3 , and ReT ($T =$ transition metal) [7–14]. The latter three also represent typical examples of noncentrosymmetric superconductors (NCSCs). In this case, the lack of space-inversion symmetry leads to an electric field gradient and hence to an antisymmetric spin-orbit coupling (ASOC), which splits the Fermi surface with opposite spin configurations. Often the strength of ASOC exceeds the superconducting energy gap, and the pairing of electrons belonging to different spin-split bands results in a mixture of singlet and triplet states. Due to such mixed pairing, NCSCs can exhibit significantly different properties from their conventional counterparts, e.g., a nodal superconducting gap [15–19], upper critical fields exceeding the Pauli limit [9,20,21], or, as recently proposed, topological superconductivity [22–24]. In turn, the structure and/or symmetry may be important in

determining the effects of ASOC on the superconducting properties [25].

In general, the breaking of time-reversal and spatial-inversion symmetries are not necessarily correlated. Indeed, many NCSCs, such as Mo_3Al_2C [26], Mo_3Rh_2N [27], $LaTSi_3$ [25,28,29], and $Mg_{10}Ir_{19}B_{16}$ [30] do not exhibit spontaneous magnetic fields in the superconducting state and hence TRS is preserved. TRS breaking in NCSCs is supposed to arise mostly from unconventional pairing mechanisms. For example, $LaNiC_2$ is proposed to be a pure nonunitary triplet SC [7,31] with pairing between the same spins in two different orbitals [32].

Despite numerous NCSCs cases, to date only a few of them are known to break TRS in their superconducting state. The causes of such selectivity remain largely unknown. Therefore, the availability of other NCSCs with broken TRS, such as Zr_3Ir reported here, would improve our understanding of the interplay between the different types of symmetry. In this Rapid Communication, we report systematic studies of Zr_3Ir by means of magnetization, transport, thermodynamic, and muon-spin relaxation/rotation (μ SR) measurements. The key observation of spontaneous magnetic fields, revealed by ZF- μ SR, indicates that Zr_3Ir represents a *structurally different member* of the NCSC family, making it a benchmark for the current theories of TRS breaking and unconventional SC in NCSCs.

Polycrystalline Zr_3Ir samples were prepared by the arc melting method [33]. The crystal structure and the sample purity were checked via x-ray powder diffraction using a

*Corresponding author: tian.shang@psi.ch†Corresponding author: S.Ghosh@kent.ac.uk

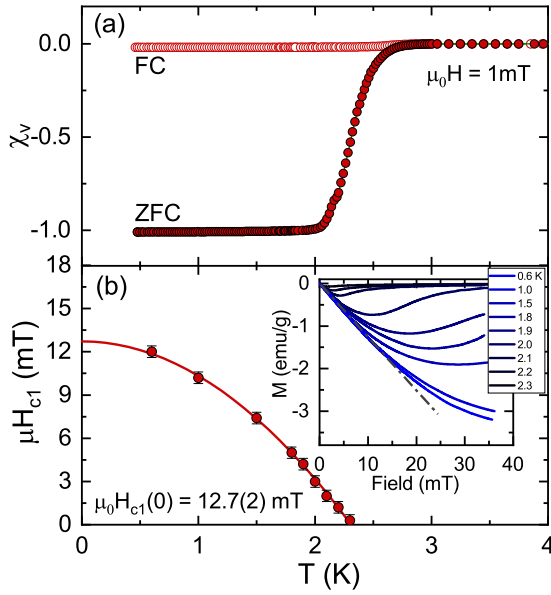


FIG. 1. (a) Temperature-dependent zero-field-cooled (ZFC) and field-cooled (FC) magnetic susceptibilities, measured in an applied field of 1 mT for Zr_3Ir . (b) Estimated $\mu_0 H_{c1}$ values vs temperature; the solid line represents a fit to $\mu_0 H_{c1}(T) = \mu_0 H_{c1}(0)[1 - (T/T_c)^2]$. The inset shows the field-dependent magnetization $M(H)$ recorded at various temperatures. $\mu_0 H_{c1}$ was identified with the deviation of $M(H)$ from linearity (dashed-dotted line).

Bruker D8 diffractometer. Consistent with previous results [34], Zr_3Ir crystallizes in a tetragonal $\alpha\text{-V}_3\text{S}$ -type noncentrosymmetric structure with space group $I42m$ (121) [33]. The magnetic susceptibility, electrical resistivity, and heat capacity measurements were performed on a Quantum Design magnetic and physical property measurement system. The μSR measurements were carried out on the GPS and LTF spectrometers of the πM3 beam line at the Paul Scherrer Institut (PSI), Villigen, Switzerland.

As shown in Fig. 1(a), the magnetic susceptibility indicates the SC onset at 2.7 K, consistent with electrical resistivity data [33]. The splitting of FC and ZFC susceptibilities is typical of type-II superconductors. To determine H_{c1} , the field-dependent magnetization $M(H)$ was measured at various temperatures, as shown in the inset of Fig. 1(b). The solid line in Fig. 1(b) is a fit to $\mu_0 H_{c1}(T) = \mu_0 H_{c1}(0)[1 - (T/T_c)^2]$, which provides a lower critical field 12.7(1) mT and $T_c = 2.3$ K. The bulk SC of Zr_3Ir was further confirmed by heat capacity measurements [33].

To explore the SC of Zr_3Ir at a microscopic level, we resort to transverse field (TF) μSR measurements. Here, a FC protocol is used to induce a flux-line lattice (FLL) in the mixed superconducting state. The optimal field value for such experiments was determined via preliminary field-dependent μSR measurements [33]. Figure 2(a) shows typical TF- μSR spectra, collected above and below T_c at 30 mT. The asymmetry of TF- μSR spectra is described by

$$A_{\text{TF}} = A_s e^{-\sigma^2 t^2/2} \cos(\gamma_\mu B_s t + \phi) + A_{\text{bg}} \cos(\gamma_\mu B_{\text{bg}} t + \phi). \quad (1)$$

Here, A_s (88%) and A_{bg} (12%) are the sample and background asymmetries, with the latter not undergoing any depolar-

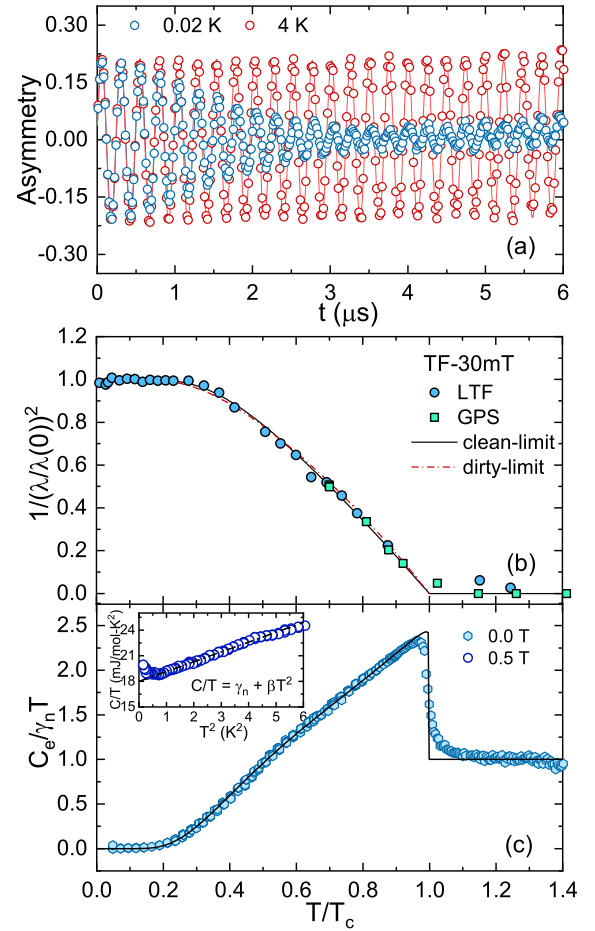


FIG. 2. (a) Time-domain TF- μSR spectra in the superconducting (0.02 K) and the normal (4 K) phase of Zr_3Ir measured in a field of $\mu_0 H_{\text{appl}} = 30$ mT. (b) Normalized superfluid density and (c) zero-field electronic specific heat vs the reduced temperature (T/T_c). The μSR data sets collected on GPS and LTF spectrometers are highly consistent. The inset in (c) shows the raw C/T data measured in a 0.5-T applied field as a function of T^2 . The dashed line is a fit to $C/T = \gamma_n + \beta T^2$, from which the phonon contribution was evaluated. The solid black lines in (b) and (c) represent fits using a fully gapped s -wave model, while the red dashed-dotted line in (b) is a fit to a dirty-limit model.

ization. $\gamma_\mu/2\pi = 135.53$ MHz/T is the muon gyromagnetic ratio, B_s and B_{bg} are the local fields sensed by implanted muons in the sample and the background (e.g., sample holder), ϕ is a shared initial phase, and σ is a Gaussian relaxation rate reflecting the field distribution inside the sample.

In the superconducting state, σ includes contributions from both the FLL (σ_{sc}) and a smaller, temperature-independent relaxation, due to nuclear moments (σ_n). The former can be extracted by subtracting the nuclear contribution in quadrature, i.e., $\sigma_{\text{sc}} = \sqrt{\sigma^2 - \sigma_n^2}$. Since the upper critical field H_{c2} of Zr_3Ir is relatively modest (0.62 T) [33], to extract the magnetic penetration depth λ_{eff} from the measured σ_{sc} we had to consider the expression [35,36]

$$\sigma_{\text{sc}}(h) = 0.172 \frac{\gamma_\mu \Phi_0}{2\pi} (1-h) [1 + 1.21(1-\sqrt{h})^3] \lambda_{\text{eff}}^{-2}, \quad (2)$$

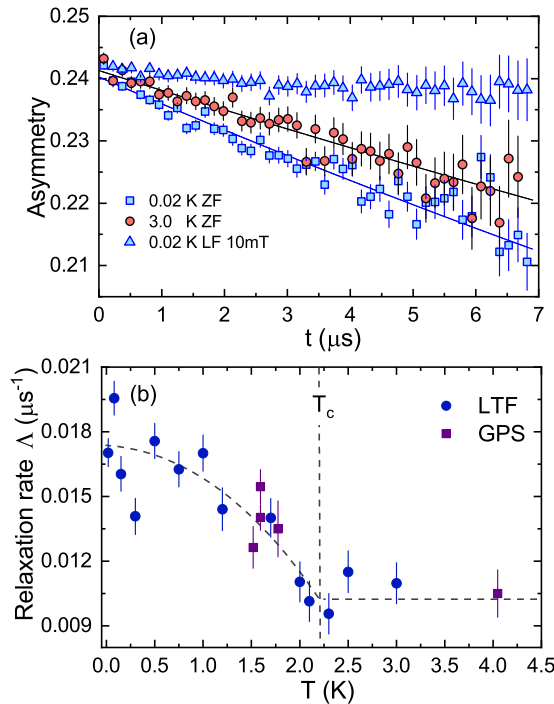


FIG. 3. Representative zero-field μ SR spectra in the superconducting (0.02 K) and the normal (3 K) phase of Zr_3Ir , together with longitudinal field data, collected at 0.02 K and 10 mT. The solid lines are fits to Eq. (3). (b) Derived relaxation rate Δ vs temperature. The dashed lines are guides to the eye. The data sets collected on GPS and LTF spectrometers are highly consistent.

valid for intermediate values of the reduced magnetic field, $h = H_{\text{appl}}/H_{c2}$. Figure 2(b) shows the normalized superfluid density ($\rho_{\text{sc}} \propto 1/\lambda^2$) versus the reduced temperature T/T_c for Zr_3Ir . For $T < 0.3T_c$, the superfluid density is nearly temperature independent, indicating the absence of residual low- T excitations and hence a fully gapped superconducting state. The temperature-dependent superfluid density was fitted by using a fully gapped s -wave model with a single superconducting gap, which provides $\Delta(0) = 0.30(1)$ meV and $\lambda(0) = 294(2)$ nm. The coherence length ξ_0 is slightly larger than the electronic mean free path l_e (see Table SIII in the Supplemental Material), implying that Zr_3Ir is a superconductor in the dirty limit. Thus, similar to other NCSCs [37], the temperature dependence of its superfluid density was also analyzed by a dirty-limit model, which yields a gap value of $0.23(1)$ meV, slightly smaller than the clean-limit value, but consistent with previous studies [38].

The zero-field specific-heat data after subtracting the phonon βT^2 contribution [see the inset in Fig. 2(c)] are shown in Fig. 2(c). The fit (solid line) yields a Sommerfeld coefficient $\gamma_n = 17.9$ mJ mol $^{-1}$ K $^{-2}$ and a single isotropic gap, $\Delta(0) = 0.32(1)$ meV. Thus, both specific-heat and TF- μ SR results are compatible with a *fully gapped* superconducting state.

ZF- μ SR measurements were used to establish the onset of TRS breaking in the superconducting state through its key signature, the appearance of spontaneous magnetic fields below T_c . Representative ZF- μ SR spectra, shown in Fig. 3(a), indicate a clear change in the muon-spin relaxation between

3 and 0.02 K. For nonmagnetic materials, in the absence of applied fields, the depolarization of muon spins is mainly determined by the randomly oriented nuclear moments. This behavior is normally described by a Gaussian Kubo-Toyabe relaxation function [39,40], as in the case of Re-based NCSCs [9–13]. For Zr_3Ir , the depolarization shown in Fig. 3 is more consistent with a Lorentzian decay. Indeed, attempts to analyze the data with a combined Gaussian and Lorentzian Kubo-Toyabe function, as in Refs. [9,10], systematically exclude the Gaussian component. This suggests that the fields sensed by the implanted muons arise from the diluted (and tiny) nuclear moments present in Zr_3Ir . Thus, the solid lines in Fig. 3(a) are fits to a Lorentzian Kubo-Toyabe relaxation function

$$A_{\text{ZF}} = A_s \left\{ \frac{1}{3} + \frac{2}{3}(1 - \Delta t)e^{-\Delta t} \right\} + A_{\text{bg}}. \quad (3)$$

Here, A_s and A_{bg} are the same as in the TF- μ SR case [see Eq. (1)]. The derived muon-spin relaxation rate Δ versus temperature is summarized in Fig. 3(b). Its relative change is comparable to that in other NCSCs with broken TRS [7–14], and $\Delta(T)$ shows a distinct increase below T_c , while being almost temperature independent above T_c . Such an increase in the muon-spin relaxation rate below T_c was also found in other compounds, e.g., La_7Ir_3 , LaNiC_2 , and Sr_2RuO_4 [3,7,8]. This provides unambiguous evidence that TRS is also broken in the superconducting state of Zr_3Ir . We note that, due to insufficient time resolution, a previous study reported standard deviations in $\Delta(T)$ of ~ 0.01 μs^{-1} [38]. Consequently, it could not capture the small yet systematic increase in $\Delta(T)$, less than ~ 0.008 μs^{-1} , shown in Fig. 3(b) [33]. To rule out the possibility of extrinsic effects related to a defect- or impurity-induced relaxation at low temperatures, we also carried out auxiliary longitudinal-field μ SR measurements at the base temperature (0.02 K). As shown in Fig. 3(a), a small 10-mT field is sufficient to lock the muon spins and hence to fully decouple them from the weak spontaneous magnetic fields. This further supports the intrinsic nature of TRS breaking in the superconducting state of Zr_3Ir .

To date, TRS breaking has been encountered only in three structurally different NCSCs: the CeNiC $_2$ -type LaNiC_2 [7], the α -Mn-type ReT [9–13], and the Th $_7\text{Fe}_3$ -type La_7T_3 [8,14]. With the α -V $_3\text{S}$ -type Zr_3Ir reported here, we show the TRS breaking to occur in a *structurally different* NCSC class. However, we point out that while the crystal structure might influence TRS breaking in NCSCs, its role is not well known. Thus, many NCSCs, e.g., $\text{Mo}_3\text{Al}_2\text{C}$, $\text{Mo}_3\text{Rh}_2\text{N}$, LaTSi_3 , $\text{Mg}_{10}\text{Ir}_{19}\text{B}_{16}$, and $\text{Nb}_{0.5}\text{Os}_{0.5}$ [25–27,29,30,41], preserve TRS, although the last two share the same α -Mn-type structure with other TRS breaking ReT NCSCs. Moreover, the triplet pairing component appears to have a negligible effect in the properties of these NCSCs. Finally, in some of NCSCs, such as Re_3W [10,42], changes in muon-spin relaxation below T_c may be below the resolution of the μ SR technique.

To gain insight into the structure of the superconducting order parameter in Zr_3Ir , we performed electronic band-structure calculations and symmetry analysis of the Ginzburg-Landau (GL) free energy [1,43]. The band structures, both with and without SOC, were calculated by means of density-functional theory (DFT) within the generalized gradient

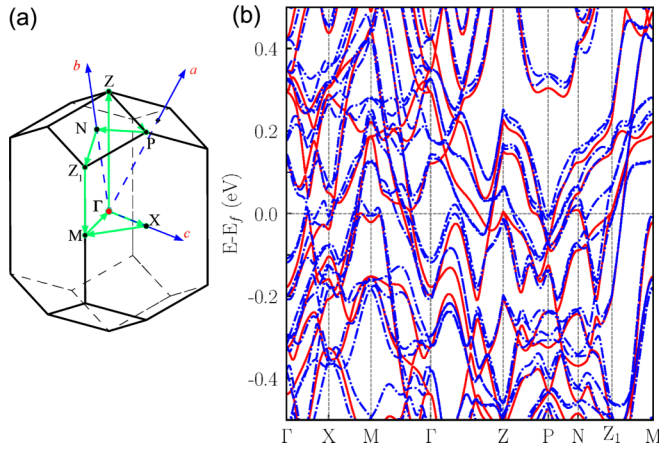


FIG. 4. (a) High-symmetry points of the Zr₃Ir unit cell. (b) Electronic band structure with (dotted blue lines) and without SOC (solid red lines), within ± 0.5 eV from the Fermi energy.

approximation (GGA) [33,44–48] and are shown in Fig. 4. The estimated band splitting near the Fermi level due to the ASOC, which plays an important role in determining the superconducting properties, is about 100 meV. While it is comparable to that of NCSCs, such as PdBiSe (~ 109 meV) [49] and K₂Cr₃As₃ (~ 60 meV) [50], it is much smaller than that of CePt₃Si (~ 200 meV) [51] and Li₂Pt₃B (~ 200 meV) [52]. The band structure shown in Fig. 4(b) also reveals multiple dispersive bands crossing the Fermi energy. In particular, the electron pockets centered around the Γ point are much larger than the hole pockets centered around the Z point.

The space group of Zr₃Ir, $I\bar{4}2m$, is symmorphic (direct product of the corresponding point group D_{2d} and the group of crystalline translations). Hence, the uniform superconducting instabilities of Zr₃Ir are fully determined by the normal-state symmetry group $\mathcal{G} = G \otimes U(1) \otimes \mathcal{T}$, where G is the group of point symmetries and spin rotations, and \mathcal{T} is the group of TRS. The GL free energy of the system must be invariant under \mathcal{G} , which has the same spatial symmetry as D_{2d} having four one-dimensional (1D) and one two-dimensional (2D) irreducible representations (irreps). The presence of the 2D irrep allows for a two-component superconducting order parameter in Zr₃Ir, while a nontrivial phase difference between them may lead to TRS breaking. Note that SC in this channel requires additional crystalline symmetry breaking and hence the pairing mechanism is necessarily *unconventional* (i.e., not phonon mediated).

SOC has dramatic consequences on the pairing symmetry of Zr₃Ir due to noncentrosymmetry and its relatively large band splitting (see Fig. 4). When SOC cannot be neglected, the superconducting state is, in general, a mixture of singlets and triplets. The only possible order parameter breaking TRS in this case is $\hat{\Delta}(\mathbf{k}) = [\Delta_0(\mathbf{k}) + \mathbf{d}(\mathbf{k}) \cdot \boldsymbol{\sigma}]i\sigma_y$, where $\Delta_0(\mathbf{k}) = A_1(k_x + ik_y)k_z$ is the singlet component and $\mathbf{d}(\mathbf{k}) = [A_2k_z, iA_2k_x, B_2(k_x + ik_y)]$ is the triplet component (the full derivation is given in the Supplemental Material). Here, $\boldsymbol{\sigma} = \{\sigma_x, \sigma_y, \sigma_z\}$ are the Pauli matrices and A_1 , A_2 , and B_2 are constants independent of \mathbf{k} . When $|A_2|, |B_2| \ll |A_1|$, the limit of weak SOC is recovered.

Now, we discuss the compatibility of the above order parameter with the fully gapped SC observed in Zr₃Ir. First, we consider the cases of a singlet- or triplet-dominated order parameter. A singlet-dominated TRS breaking order parameter ($A_2, B_2 \approx 0$) leads to an energy gap $|A_1||k_z|\sqrt{k_x^2 + k_y^2}$. It has a line node at the “equator” for $k_z = 0$ and two point nodes at the “north” and “south” poles. Similarly, a triplet-dominated TRS breaking order parameter ($A_1 \approx 0$) corresponds to an energy gap $[g(k_x, k_y) + 2A_2^2k_z^2 - 2|A_2||k_z|\sqrt{g(k_x, k_y) + A_2^2k_z^2}]^{1/2}$, where $g(k_x, k_y) = B_2^2(k_x^2 + k_y^2)$. This instability also has two point nodes at the two poles, but no line nodes (see the respective gap plots in the Supplemental Material). In the general case, where both singlet and triplet components are significant, we compute the excitation spectrum numerically, by using the Bogoliubov–de Gennes formalism [1]. We use the simplest form of the normal-state band structure and ASOC coupling constant compatible with the crystal symmetry [33]. As soon as a triplet component is present, the line node at the “equator” is gapped out. In contrast, the “north” and “south” point nodes are present throughout the phase diagram.

The above results are based only on symmetry arguments considering a generic Fermi surface. To adapt them to Zr₃Ir, we consider its Fermi surfaces which contribute the most to the density of states at the Fermi level (computed using DFT [33]). They are *open* at the two poles [33], implying that a fully gapped behavior is expected for TRS breaking order parameters with a non-negligible triplet component. Note that an equatorial line node for a singlet-dominated SC order parameter necessarily gives rise to a gapless spectrum for the given Fermi-surface topology. Therefore, to reproduce the fully gapped spectrum of Zr₃Ir, a triplet component (possibly small) induced by SOC is essential.

The specific-heat jump at T_c ($\Delta C/\gamma T_c \sim 1.32$) and the gap to the critical-temperature ratio ($2\Delta/k_B T_c \sim 3.24$) of Zr₃Ir shown in Fig. 2 seem to suggest a singlet, phonon-mediated SC. This raises the question of how such a conventional mechanism may lead to a state with broken TRS, corresponding to a nontrivial irrep of the crystal point group. Recently, it was proposed that in multiband systems, whose bands derive from distinct but symmetry-related sites within the unit cell, this may be achieved by a loop supercurrent state [53]. Interestingly, such conditions are satisfied in Zr₃Ir. In this picture, the k -dependent order parameter comes from a real-space pairing potential: $|\Delta\rangle = |1\rangle + i|2\rangle$, where $|1\rangle = (0, 0, -1, 1)$ and $|2\rangle = (-1, 1, 0, 0)$ are real-space basis functions giving the on-site, singlet pairing strength in each of the four symmetry-related sites within the unit cell [33]. This ground state has finite currents within a unit cell spontaneously breaking TRS at T_c [53]. Note that the energy of this superconducting instability is driven by singlet pairing, while the additional triplet contribution is induced by SOC.

Finally, for weak SOC, $G = D_{2d} \otimes SO(3)$, with D_{2d} and $SO(3)$ acting independently. Hence, G can have one-, two-, three-, and six-dimensional irreps. As a result, additional TRS breaking SC states may appear, including those arising from a pure $SO(3)$ pairing, as proposed for LaNiC₂ and LaNiGa₂ [6,7,31].

In conclusion, we have discovered a *structurally different* member of the NCSC class, Zr_3Ir , which breaks time-reversal symmetry at the superconducting transition. The spontaneous magnetic fields appearing below T_c were detected by ZF- μ SR, while its electronic properties were investigated by means of magnetization, transport, thermodynamic, and μ SR measurements. Both the zero-field specific heat and superfluid density (from TF- μ SR) reveal a single, fully gapped superconducting state in Zr_3Ir . Theoretically, we obtain a superconducting order parameter which is fully compatible with the observations. Considering its different structure from the known NCSCs, Zr_3Ir is expected to stimulate further studies on the

interplay of space, time, and gauge symmetries in establishing the unique properties of NCSCs.

This work was supported by the Schweizerische Nationalfonds zur Förderung der Wissenschaftlichen Forschung (SNF) (Grants No. 200021_169455 and No. 206021_139082). S.K.G. and J.Q. are supported by EPSRC through the project “Unconventional superconductors: New paradigms for new materials” (Grant No. EP/P00749X/1). L.J.C. thanks MOST for the funding under Projects No. 104-2112-M-006-010-MY3 and No. 107-2112-M-006-020. Finally, we acknowledge the assistance from S μ S beamline scientists at PSI.

-
- [1] M. Sigrist and K. Ueda, Phenomenological theory of unconventional superconductivity, *Rev. Mod. Phys.* **63**, 239 (1991).
- [2] C. C. Tsuei and J. R. Kirtley, Pairing symmetry in cuprate superconductors, *Rev. Mod. Phys.* **72**, 969 (2000).
- [3] G. M. Luke, Y. Fudamoto, K. M. Kojima, M. I. Larkin, J. Merrin, B. Nachumi, Y. J. Uemura, Y. Maeno, Z. Q. Mao, Y. Mori, H. Nakamura, and M. Sigrist, Time-reversal symmetry-breaking superconductivity in Sr_2RuO_4 , *Nature (London)* **394**, 558 (1998).
- [4] Y. Aoki, A. Tsuchiya, T. Kanayama, S. R. Saha, H. Sugawara, H. Sato, W. Higemoto, A. Koda, K. Ohishi, K. Nishiyama, and R. Kadono, Time-Reversal Symmetry-Breaking Superconductivity in Heavy-Fermion $PrOs_4Sb_{12}$ Detected by Muon-Spin Relaxation, *Phys. Rev. Lett.* **91**, 067003 (2003).
- [5] G. M. Luke, A. Keren, L. P. Le, W. D. Wu, Y. J. Uemura, D. A. Bonn, L. Taillefer, and J. D. Garrett, Muon Spin Relaxation in UPt_3 , *Phys. Rev. Lett.* **71**, 1466 (1993).
- [6] A. D. Hillier, J. Quintanilla, B. Mazidian, J. F. Annett, and R. Cywinski, Nonunitary Triplet Pairing in the Centrosymmetric Superconductor $LaNiGa_2$, *Phys. Rev. Lett.* **109**, 097001 (2012).
- [7] A. D. Hillier, J. Quintanilla, and R. Cywinski, Evidence for Time-Reversal Symmetry Breaking in the Noncentrosymmetric Superconductor $LaNiC_2$, *Phys. Rev. Lett.* **102**, 117007 (2009).
- [8] J. A. T. Barker, D. Singh, A. Thamizhavel, A. D. Hillier, M. R. Lees, G. Balakrishnan, D. McK. Paul, and R. P. Singh, Unconventional Superconductivity in La_7Ir_3 Revealed by Muon Spin Relaxation: Introducing a New Family of Noncentrosymmetric Superconductor that Breaks Time-Reversal Symmetry, *Phys. Rev. Lett.* **115**, 267001 (2015).
- [9] T. Shang, G. M. Pang, C. Baines, W. B. Jiang, W. Xie, A. Wang, M. Medarde, E. Pomjakushina, M. Shi, J. Mesot, H. Q. Yuan, and T. Shiroka, Nodeless superconductivity and time-reversal symmetry breaking in the noncentrosymmetric superconductor $Re_{24}Ti_5$, *Phys. Rev. B* **97**, 020502(R) (2018).
- [10] T. Shang, M. Smidman, S. K. Ghosh, C. Baines, L. J. Chang, D. J. Gawryluk, J. A. T. Barker, R. P. Singh, D. McK. Paul, G. Balakrishnan, E. Pomjakushina, M. Shi, M. Medarde, A. D. Hillier, H. Q. Yuan, J. Quintanilla, J. Mesot, and T. Shiroka, Time-Reversal Symmetry Breaking in Re-Based Superconductors, *Phys. Rev. Lett.* **121**, 257002 (2018).
- [11] R. P. Singh, A. D. Hillier, B. Mazidian, J. Quintanilla, J. F. Annett, D. McK. Paul, G. Balakrishnan, and M. R. Lees, Detection of Time-Reversal Symmetry Breaking in the Noncentrosymmetric Superconductor Re_6Zr using Muon-Spin Spectroscopy, *Phys. Rev. Lett.* **112**, 107002 (2014).
- [12] D. Singh, J. A. T. Barker, A. Thamizhavel, D. McK. Paul, A. D. Hillier, and R. P. Singh, Time-reversal symmetry breaking in the noncentrosymmetric superconductor Re_6Hf : Further evidence for unconventional behavior in the α -Mn family of materials, *Phys. Rev. B* **96**, 180501(R) (2017).
- [13] D. Singh, S. K. P., J. A. T. Barker, D. McK. Paul, A. D. Hillier, and R. P. Singh, Time-reversal symmetry breaking in the noncentrosymmetric superconductor Re_6Ti , *Phys. Rev. B* **97**, 100505(R) (2018).
- [14] D. Singh, M. S. Scheurer, A. D. Hillier, and R. P. Singh, Time-reversal-symmetry breaking and unconventional pairing in the noncentrosymmetric superconductor La_7Rh_3 probed by μ SR, [arXiv:1802.01533](https://arxiv.org/abs/1802.01533).
- [15] H. Q. Yuan, D. F. Agterberg, N. Hayashi, P. Badica, D. Vandervelde, K. Togano, M. Sigrist, and M. B. Salamon, *s*-Wave Spin-Triplet Order in Superconductors without Inversion Symmetry: Li_2Pd_3B and Li_2Pt_3B , *Phys. Rev. Lett.* **97**, 017006 (2006).
- [16] M. Nishiyama, Y. Inada, and G.-q. Zheng, Spin triplet superconducting state due to broken inversion symmetry in Li_2Pt_3B , *Phys. Rev. Lett.* **98**, 047002 (2007).
- [17] I. Bonalde, W. Brämer-Escamilla, and E. Bauer, Evidence for Line Nodes in the Superconducting Energy Gap of Noncentrosymmetric $CePt_3Si$ from Magnetic Penetration Depth Measurements, *Phys. Rev. Lett.* **94**, 207002 (2005).
- [18] G. M. Pang, M. Smidman, W. B. Jiang, J. K. Bao, Z. F. Weng, Y. F. Wang, L. Jiao, J. L. Zhang, G. H. Cao, and H. Q. Yuan, Evidence for nodal superconductivity in quasi-one-dimensional $K_2Cr_3As_3$, *Phys. Rev. B* **91**, 220502(R) (2015).
- [19] D. T. Adroja, A. Bhattacharyya, M. Telling, Yu. Feng, M. Smidman, B. Pan, J. Zhao, A. D. Hillier, F. L. Pratt, and A. M. Strydom, Superconducting ground state of quasi-one-dimensional $K_2Cr_3As_3$ investigated using μ SR measurements, *Phys. Rev. B* **92**, 134505 (2015).
- [20] E. Bauer, G. Hilscher, H. Michor, C. Paul, E. W. Scheidt, A. Gribanov, Y. Seropegin, H. Noël, M. Sigrist, and P. Rogl, Heavy Fermion Superconductivity and Magnetic Order in Noncentrosymmetric $CePt_3Si$, *Phys. Rev. Lett.* **92**, 027003 (2004).
- [21] E. M. Carnicom, W. W. Xie, T. Klimczuk, J. J. Lin, K. Górnicka, Z. Sobczak, N. P. Ong, and R. J. Cava, $TaRh_2B_2$ and $NbRh_2B_2$: Superconductors with a chiral noncentrosymmetric crystal structure, *Sci. Adv.* **4**, eaar7969 (2018).
- [22] M. N. Ali, Q. D. Gibson, T. Klimczuk, and R. J. Cava, Noncentrosymmetric superconductor with a bulk three-dimensional

- Dirac cone gapped by strong spin-orbit coupling, *Phys. Rev. B* **89**, 020505(R) (2014).
- [23] Z. X. Sun, M. Enayat, A. Maldonado, C. Lithgow, E. Yelland, D. C. Peets, A. Yaresko, A. P. Schnyder, and P. Wahl, Dirac surface states and nature of superconductivity in noncentrosymmetric BiPd, *Nat. Commun.* **6**, 6633 (2015).
- [24] H. Kim, K. Wang, Y. Nakajima, R. Hu, S. Ziemak, P. Syers, L. Wang, H. Hodovanets, J. D. Denlinger, P. M. R. Brydon, D. F. Agterberg, M. A. Tanatar, R. Prozorov, and J. Paglione, Beyond triplet: Unconventional superconductivity in a spin-3/2 topological semimetal, *Sci. Adv.* **4**, eaao4513 (2018).
- [25] V. K. Anand, D. Britz, A. Bhattacharyya, D. T. Adroja, A. D. Hillier, A. M. Strydom, W. Kockelmann, B. D. Rainford, and K. A. McEwen, Physical properties of noncentrosymmetric superconductor LaIrSi₃: A μ SR study, *Phys. Rev. B* **90**, 014513 (2014).
- [26] E. Bauer, G. Rogl, X.-Q. Chen, R. T. Khan, H. Michor, G. Hilscher, E. Royanian, K. Kumagai, D. Z. Li, Y. Y. Li, R. Podloucky, and P. Rogl, Unconventional superconducting phase in the weakly correlated noncentrosymmetric Mo₃Al₂C compound, *Phys. Rev. B* **82**, 064511 (2010).
- [27] T. Shang, W. Wei, C. Baines, J. L. Zhang, H. F. Du, M. Medarde, M. Shi, J. Mesot, and T. Shiroka, Nodeless superconductivity in the noncentrosymmetric Mo₃Rh₂N superconductor: A μ SR study, *Phys. Rev. B* **98**, 180504(R) (2018).
- [28] V. K. Anand, A. D. Hillier, D. T. Adroja, A. M. Strydom, H. Michor, K. A. McEwen, and B. D. Rainford, Specific heat and μ SR study on the noncentrosymmetric superconductor LaRhSi₃, *Phys. Rev. B* **83**, 064522 (2011).
- [29] M. Smidman, A. D. Hillier, D. T. Adroja, M. R. Lees, V. K. Anand, R. P. Singh, R. I. Smith, D. McK. Paul, and G. Balakrishnan, Investigations of the superconducting states of noncentrosymmetric LaPdSi₃ and LaPtSi₃, *Phys. Rev. B* **89**, 094509 (2014).
- [30] A. A. Aczel, T. J. Williams, T. Goko, J. P. Carlo, W. Yu, Y. J. Uemura, T. Klimczuk, J. D. Thompson, R. J. Cava, and G. M. Luke, Muon spin rotation/relaxation measurements of the noncentrosymmetric superconductor Mg₁₀Ir₁₉B₁₆, *Phys. Rev. B* **82**, 024520 (2010).
- [31] J. Quintanilla, A. D. Hillier, J. F. Annett, and R. Cywinski, Relativistic analysis of the pairing symmetry of the noncentrosymmetric superconductor LaNiC₂, *Phys. Rev. B* **82**, 174511 (2010).
- [32] Z. F. Weng, J. L. Zhang, M. Smidman, T. Shang, J. Quintanilla, J. F. Annett, M. Nicklas, G. M. Pang, L. Jiao, W. B. Jiang, Y. Chen, F. Steglich, and H. Q. Yuan, Two-Gap Superconductivity in LaNiGa₂ with Nonunitary Triplet Pairing and Even Parity Gap Symmetry, *Phys. Rev. Lett.* **117**, 027001 (2016).
- [33] See the Supplemental Material at <http://link.aps.org/supplemental/10.1103/PhysRevB.102.020503> for details on the measurements of the crystal structure, electrical resistivity, heat capacity, and critical field, as well as for the data analysis, DFT calculation, and symmetry analysis.
- [34] K. Cenxual and E. Parthié, Zr₃Ir with tetragonal α -V₃S structure, *Acta Crystallogr., Sect. C* **41**, 820 (1985).
- [35] W. Barford and J. M. F. Gunn, The theory of the measurement of the London penetration depth in uniaxial type II superconductors by muon spin rotation, *Physica C* **156**, 515 (1988).
- [36] E. H. Brandt, Properties of the ideal Ginzburg-Landau vortex lattice, *Phys. Rev. B* **68**, 054506 (2003).
- [37] B. A. Frandsen, S. C. Cheung, T. Goko, L. Liu, T. Medina, T. S. J. Munsie, G. M. Luke, P. J. Baker, M. P. Jimenez S., G. Eguchi, S. Yonezawa, Y. Maeno, and Y. J. Uemura, Superconducting properties of noncentrosymmetric superconductor CaIrSi₃ investigated by muon spin relaxation and rotation, *Phys. Rev. B* **91**, 014511 (2015), and references therein.
- [38] S. K. P., D. Singh, P. K. Biswas, G. B. G. Stenning, A. D. Hillier, and R. P. Singh, Investigations of the superconducting ground state of Zr₃Ir: Introducing a new noncentrosymmetric superconductor, *Phys. Rev. Materials* **3**, 104802 (2019).
- [39] R. Kubo and T. Toyabe, in *Magnetic Resonance and Relaxation*, edited by R. Blinc (North-Holland, Amsterdam, 1967).
- [40] A. Yaouanc and P. Dalmass de Réotier, *Muon Spin Rotation, Relaxation, and Resonance: Applications to Condensed Matter* (Oxford University Press, Oxford, UK, 2011).
- [41] D. Singh, J. A. T. Barker, T. Arumugam, A. D. Hillier, D. McK. Paul, and R. P. Singh, Superconducting properties and μ SR study of the noncentrosymmetric superconductor Nb_{0.5}Os_{0.5}, *J. Phys.: Condens. Matter* **30**, 075601 (2018).
- [42] P. K. Biswas, A. D. Hillier, M. R. Lees, and D. McK. Paul, Comparative study of the centrosymmetric and noncentrosymmetric superconducting phases of Re₃W using muon spin spectroscopy and heat capacity measurements, *Phys. Rev. B* **85**, 134505 (2012).
- [43] J. F. Annett, Symmetry of the order parameter for high-temperature superconductivity, *Adv. Phys.* **39**, 83 (1990).
- [44] J. P. Perdew, K. Burke, and M. Ernzerhof, Generalized Gradient Approximation Made Simple, *Phys. Rev. Lett.* **77**, 3865 (1996).
- [45] G. Kresse and J. Furthmüller, Efficient iterative schemes for *ab initio* total-energy calculations using a plane-wave basis set, *Phys. Rev. B* **54**, 11169 (1996).
- [46] G. Kresse and J. Furthmüller, Efficiency of *ab-initio* total energy calculations for metals and semiconductors using a plane-wave basis set, *Comput. Mater. Sci.* **6**, 15 (1996).
- [47] G. Kresse and D. Joubert, From ultrasoft pseudopotentials to the projector augmented-wave method, *Phys. Rev. B* **59**, 1758 (1999).
- [48] P. E. Blöchl, Projector augmented-wave method, *Phys. Rev. B* **50**, 17953 (1994).
- [49] M. Kakihana, A. Nakamura, A. Teruya, H. Harima, Y. Haga, M. Hedo, T. Nakama, and Y. Ōnuki, Split Fermi surface properties based on the relativistic effect in superconductor PdBiSe with the cubic chiral crystal structure, *J. Phys. Soc. Jpn.* **84**, 033701 (2015).
- [50] H. Jiang, G. H. Cao, and C. Cao, Electronic structure of quasi-one-dimensional superconductor K₂Cr₃As₃ from first-principles calculations, *Sci. Rep.* **5**, 16054 (2015).
- [51] K. V. Samokhin, E. S. Zijlstra, and S. K. Bose, CePt₃Si: An unconventional superconductor without inversion center, *Phys. Rev. B* **69**, 094514 (2004).
- [52] K.-W. Lee and W. E. Pickett, Crystal symmetry, electron-phonon coupling, and superconducting tendencies in Li₂Pd₃B and Li₂Pt₃B, *Phys. Rev. B* **72**, 174505 (2005).
- [53] S. Ghosh, J. F. Annett, and J. Quintanilla, Time-reversal symmetry breaking in superconductors through loop Josephson-current order, [arXiv:1803.02618](https://arxiv.org/abs/1803.02618).